Journal of Magnetic Resonance Open 26 (2026) 100213

Contents lists available at ScienceDirect

Journal of Magnetic Resonance Open

journal homepage: www.sciencedirect.com/journal/journal-of-magnetic-resonance-open

Research Article

# Comparison of different solvent suppression techniques for polymer characterization with a 90 MHz benchtop spectrometer

Johanna Tratz, Markus Matz, Manfred Wilhelm *

*Karlsruhe Institute of Technology (KIT), Institute for Technical Chemistry and Polymer Chemistry (ITCP), Engesserstraße 18, Karlsruhe 76131, Germany*

ARTICLE INFO

*Keywords:*
Solvent suppression
Low-field NMR
Benchtop NMR
SEC-NMR
Polymers

ABSTRACT

In NMR spectroscopy, samples are usually dissolved in deuterated solvents to avoid overlap of small analyte signals with large, protonated solvent signals. However, for reasons such as cost and widespread use, using deuterated solvents is impractical, e.g., for on-flow NMR applications, since large volumes of solvent are required. This study compares six different solvent suppression techniques: PRESATuration (PRESAT), Water suppression Enhanced through $T_1$ effects (WET), Pulsed Gradient STimulated Echo (PGSTE), 1-pulse-spoil, simple solvent subtraction, and a newly developed post-acquisition suppression method named Solvent Attenuation by Fourier Elimination (SAFE). The SAFE method is based on alternating measurements of the sample solution and the pure solvent $2^n$ times, followed by a fast Fourier transform to eliminate the solvent signals, which are constant in the first approximation. The different solvent suppression methods were compared alone and in several combinations to determine their optimum suppression efficiency. The suppression was quantified by evaluating the Analyte-to-Solvent Ratio normalized to the unsuppressed $^1$H reference spectrum ($ASR_{norm}$). Furthermore, a comparison was made between the methods concerning their suitability for polymer solutions of varying molar masses, quantification towards measurement time efficiency, repeatability, and intermediate precision. The PGSTE-SAFE combination proved to be the most efficient method for polymer samples, achieving an $ASR_{norm}$ of about 47,000. The applicability of solvent suppression methods in flow-based setups was also assessed by investigating polystyrenes in non-deuterated solvents. WET, PGSTE, and a WET-PGSTE combination were applied in online Size Exclusion Chromatography-NMR (SEC—NMR) to demonstrate their potential for efficient solvent suppression in this context.

## 1. Introduction

NMR spectroscopy is a widely used and powerful technique for characterizing macromolecules, providing detailed information on their molecular structure, chemical composition, topology, molar masses, and dynamic properties in bulk or solution [1–3]. Although NMR offers a vast amount of information as a standalone method, a deeper understanding of structure-property relationships of polymers often requires the simultaneous acquisition of multiple analytical techniques to gain correlated information [4]. For instance, combining NMR with liquid chromatography allows for chemical composition information at each point in time during the chromatographic separation. Both Liquid-Adsorption Chromatography (LAC), which relies on adsorption-based mechanisms, and Size-Exclusion Chromatography (SEC), which separates analytes by hydrodynamic radius, have already been successfully coupled to high and low-field NMR spectroscopy [5–10]. In particular, SEC provides access to molar mass distributions and chemical dispersity of polymers, which are essential for linking material properties to molecular characteristics. By using an NMR spectrometer as a detector for SEC, it is possible to determine the monomers and quantify the relative amount during polymer elution, providing information on chemical composition distribution as a function of molar mass. This information is typically only obtainable using a multidetector SEC system and polymer-specific detector calibration.

Although chromatography coupled with high-field NMR was introduced over four decades ago [5], it never became widely used. The high acquisition and operating costs of high-field spectrometers (nowadays up to 28 Tesla and 1.2 GHz $^1$H Larmor frequency) and the requirement for extensive, specialized laboratory infrastructure are limitations to the widespread accessibility of high-field spectrometers combined with chromatography. Such implementations using high-field spectrometers and/or deuterated solvents were considered not feasible for SEC—NMR

* Corresponding author.
*E-mail address:* manfred.wilhelm@kit.edu (M. Wilhelm).

https://doi.org/10.1016/j.jmro.2025.100213

Available online 19 December 2025

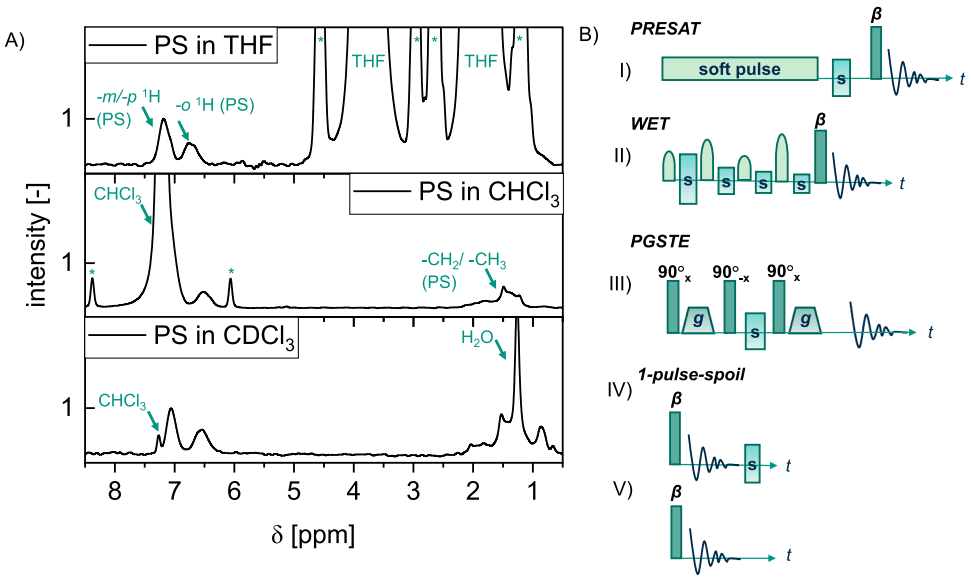


**Fig. 1.** (A) $^{1}$H spectra of 12 kg·mol$^{-1}$ Polystyrene (PS) in THF, $CHCl_3$, or $CDCl_3$ without solvent suppression, measured on a 90 MHz benchtop NMR spectrometer. The spectra are normalized to the intensity of the aromatic *m/p*-protons of PS at 7.1 ppm. $^{13}$C satellites of THF or $CHCl_3$ are indicated with asterisks. (B) Used pulse sequences: (I) PRESATuration (PRESAT), (II) Water suppression Enhanced through $T_1$ effects (WET), (III) Pulsed Gradient Stimulated Echo (PGSTE), (IV) 1-pulse-spoil. (V) $^{1}$H NMR (no suppression, and for post-acquisition solvent subtraction and Solvent Attenuation by Fourier Elimination (SAFE)). The $\beta$ readout pulse refers to a defined excitation angle $\beta$, here $\beta = 90°$ The "s"-pulse corresponds to a spoil pulse, the "g"-pulse corresponds to a gradient pulse.

applications in industry [11].

In contrast, low-field or benchtop NMR spectrometers with permanent magnets from 0.5–2.9 T, resulting in 20–125 MHz $^{1}$H Larmor frequency, have been commercially available since the early 2010s [12]. These spectrometers have a compact design (<0.5 m in all directions, mass < 100 kg) and require no cryogenic liquids (helium and/or nitrogen) for cooling the magnet. The number of applications and publications is continually increasing as they offer a more affordable, space-efficient alternative. This makes NMR spectroscopy more accessible to a broader audience and brings NMR back onto laboratory benches.

Additionally, benchtop spectrometers are far more suitable for hyphenation with other analytical instruments or on-flow reaction or process monitoring. Furthermore, the often implemented external $^{19}$F lock systems in benchtop spectrometers eliminate the need for deuterated solvents [13].

Liquid NMR measurements in 5 mm test tubes are typically performed using 1–5 mg samples diluted in <1.0 mL of deuterated solvent. This minimizes solvent signals overlapping with analyte signals and enables stable field locking via an internal deuterium lock, which is commonly integrated into high-field instruments. However, the continuous use of deuterated solvents would be cost-intensive in chromatographic coupling or for online reaction monitoring. In such cases, an external lock system offers an advantage as it enables analysis in protonated solvents under flow conditions.

Another important application of solvent suppression is the characterization of biological macromolecules, which are mainly dissolved in water. To observe exchangeable protons in protic solvents (e.g., -OH, -NH, -$NH_2$), non-deuterated solvents are required [14].

For such applications, solvent suppression is essential. Prior studies on benchtop systems have compared various solvent suppression methods, such as PRESATuration (PRESAT), Water suppression Enhanced through $T_1$ effects (WET), excitation sculpting-based, and binomially selective pulse sequences, for small molecules. Gouilleux et al., for example, investigated gradient-based methods using a 43.6 MHz NMR spectrometer, finding the WET-180-NOESY pulse sequence to be highly effective under static and flow conditions when using alanine and lactate model systems [15]. Pellizzari et al. systematically compared binomial pulse schemes versus PRESAT-based sequences at 80 MHz using "real-world" matrices (e.g., human urine samples and energy drinks). They concluded that PRESAT is sufficient for high analyte concentrations, whereas low-concentrated samples benefit from more sophisticated binomial schemes for solvent suppression [16]. The Wilhelm group has previously investigated WET, jump-and-return, 1-pulse-spoil, and Water Eliminated Fourier Transform (WEFT) suppression methods at 43 and 62 MHz for SEC—NMR measurements of polymeric samples and compared them towards repetition rate, solvent suppression ratios as well as baseline distortions [17].

This research will be extended in two ways here. Firstly, six suppression methods will be compared under static conditions at 90 MHz using a polystyrene model system in either THF or $CHCl_3$. The methods are PRESAT, WET, Pulsed Gradient STimulated Echo (PGSTE), 1-pulse-spoil, simple mathematical subtraction, and Solvent Attenuation by Fourier Elimination (SAFE), as well as combinations of these. SAFE is introduced here as a newly developed method that expands the range of post-acquisition suppression techniques. The solvent suppression efficiency of all methods will be quantified by their analyte-to-solvent ratio after method optimization, repeatability, intermediate precision and time efficiency. Furthermore, the molar mass dependency of various suppression methods will be discussed in detail and a practical guide to selecting the most suitable pulse sequences available on most benchtop spectrometers for different measurement conditions will be provided. Secondly, WET and PGSTE, which have been identified as the most efficient solvent suppression pulse sequences for polymers in online conditions, will be compared separately and in combination (WET-PGSTE) in SEC—NMR measurements, with the aim of optimizing solvent suppression efficiency for online chromatographic applications. This study demonstrates substantially reduced residual THF signals in 2D SEC—NMR measurements compared to previous studies by our group [17].

## 2. Theoretical background

Suppressing solvent signals in NMR spectra using protonated solvents is crucial since the solvent is usually present at much higher concentrations, typically a factor ~$10^3$, than the analyte [2]. This results

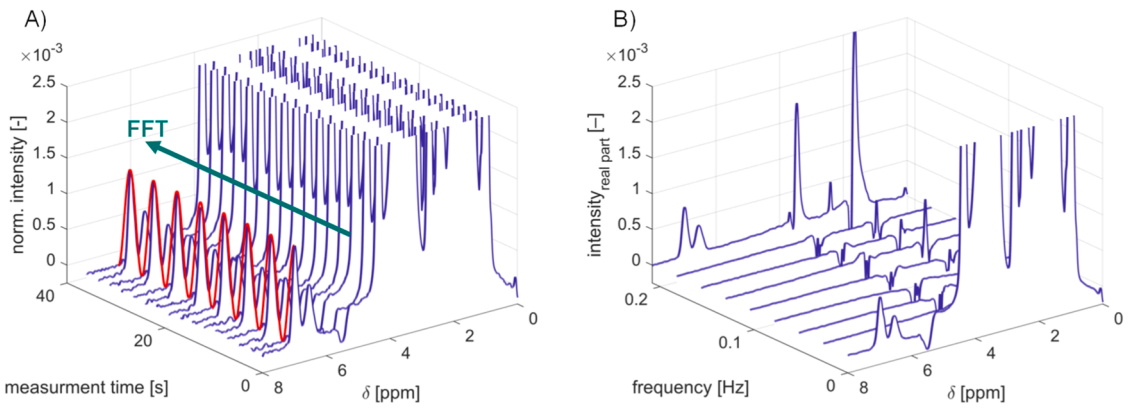


**Fig. 2.** (A) Periodic arrangement of pure THF and THF with polystyrene (PS12k, 12kg·mol$^{-1}$). The red line indicates the periodic zigzag modulation for PS12k. Spectra are normalized to the maximum solvent peak intensity at 3.6 ppm. (B) Fast Fourier transformation (FFT) at each chemical shift leads to the solvent-filtered Fourier spectrum. Only the real parts of one-half of the mirror-symmetric FT spectra are shown. The spectrum at the modulation frequency (0.21 Hz, last spectrum) is used for data evaluation, see Section 4.1.

in intense solvent signals, with broad spectral feet concealing smaller analyte peaks (see Fig. 1A). This issue is even more significant when using low-field NMR spectrometers, which have lower spectral resolution (typically 0.003 ppm) due to lower magnetic field strength compared to high-field instruments, leading to even broader line widths. Moreover, strong solvent signals may exceed the receiver's dynamic range of the Analog-to-Digital Converter (ADC), leading to baseline distortions. A reduction in Receiver Gain (RG) further lowers the digital intensity resolution of the analyte. The simultaneous detection of small analyte peaks beside strong solvent signals will thus lead to a stepped intensity representation of the low signal intensities due to digital quantization [18]. Another effect of detecting strong solvent signals is radiation damping, which is caused by strong transverse magnetization of solvent nuclei. This magnetization induces an oscillating current in the receiver coil, generating a secondary Radio Frequency (RF) field. This alters the amplitude and phase of the original RF field, effectively shortening the apparent transverse relaxation time ($T^*_2$), thereby broadening the solvent signal. The effect is significantly less pronounced at low magnetic field strengths, as it's directly related to the sample magnetization, making it less critical for benchtop NMR applications [15,19].

To address these challenges, various solvent suppression pulse sequences have already been incorporated into the standard NMR repertoire for both high-field and low-field spectrometers [3]. Generally, suppression methods are applied either before or after data acquisition [14]. Suppression techniques belonging to the first category can be further differentiated into the following [2]: (a) Methods that saturate the solvent resonance by applying long, weak RF pulses before the readout pulse, such as the PRESATuration (PRESAT) technique [20,21]; (b) methods that produce zero net excitation of the solvent, whereby the solvent spins are tilted away from the transverse detection plane while the magnetization of the desired analyte peaks is deflected to the receiver during acquisition such as jump-return sequences [22]; and (c) a third class of solvent suppression techniques involves dephasing the solvent magnetization using Pulsed Field Gradients (PFGs). Examples are Water suppression Enhanced through $T_1$ effects (WET) [23] and WATER suppression by GrAdient-Tailored Excitation (WATERGATE) [24]. Although such gradient-based techniques have been standard on high-field spectrometers since the 1990s, they could only be implemented in benchtop NMR instruments around 10 years ago with the introduction of dedicated gradient coils [25]. Before then, shim coils, which are normally intended for tuning magnetic field homogeneity, were repurposed to create weak gradient effects. The second category of post-acquisition suppression methods is either based on hardware frequency filters [26] or software post-processing procedures, alike simple solvent subtraction [14]. These methods can be applied in combination with those introduced previously.

The most commonly used method for solvent suppression in NMR spectroscopy is PRESAT, as the pulse sequence is typically incorporated into all NMR spectrometers without requiring additional equipment (e.g., gradients) [15,27]. Applying a long (e.g. 1–3 s) weak RF pulse at the beginning of the pulse sequence, which irradiates in principle as many (solvent) resonances as desired (Fig. 1B, I), can saturate and thus suppress specific frequency bands. Frequencies of the analyte resonance below or close to the solvent signal will also be suppressed. A gradient-based pulse sequence, which was designed for compensation of pulse inaccuracies and scattering of the longitudinal magnetization of the solvent for improved suppression, is the WET sequence [23]. It consists of four frequency-selective RF pulses, each of which is followed by a pulsed gradient (see Fig. 1B, II). It is significantly faster than PRESAT with a higher selectivity, making it more suitable for on-flow NMR experiments [17].

Another gradient-based method is the pulsed gradient stimulated echo (PGSTE) sequence. Zijl and Moonen first introduced this method for solvent suppression in 1990 [28]. The pulse sequence originates from diffusion NMR and is typically employed in DOSY (Diffusion-Ordered SpectroscopY) experiments. The pulse sequence includes three hard 90° RF pulses and two gradient pulses applied immediately after the first and third RF pulses (see Fig. 1B, III). Between the second and third 90° pulses, there is a variable time interval, Δ, in the 20–500 ms range, also known as "diffusion time". Smaller molecules, such as solvents, with a self-diffusion coefficient $D$ (e.g., water is ~$2{\cdot}10^{-9}$ m$^2{\cdot}$s$^{-1}$ at 25 °C [29]), diffuse substantially faster than larger molecules (e.g., synthetic polymers or proteins with $D$ in solution ranging from ~$10^{-11}$ to ~$10^{-14}$ m$^2{\cdot}$s$^{-1}$ [30–32]), causing greater dephasing by the applied gradients for the solvent molecules. The PGSTE sequence could consequently be used as a "low diffusion pass filter", suppressing fast-diffusing components while largely preserving slow-diffusing components [33]. Therefore, PGSTE-based suppression is especially suitable when there is a significant difference in $D$ or molar mass between solvent and analyte (e.g., polymers), see Section 4.1.1 for a detailed discussion.

A pulse sequence specifically designed for polymer analysis in SEC—NMR measurements is the 1-pulse-spoil method [17,34]. This sequence exploits the difference in $T_1$ between high-molar-mass molecules and low-molar-mass solvents, similar to the principle of the Water Eliminated Fourier Transform (WEFT) sequence [35]. Since macromolecules relax 3–6 times faster than solvent molecules, depending on molar mass, the pulse sequence acts as a $T_1$-filter when the repetition time ($t_{rep}$, time between two consecutive scans) is short compared to solvent $T_1$ (see Fig. 1B, IV). Please note that in chromatography, solvents and solutions are degassed before being injected into the column. Consequently, the normally dissolved $O_2$ (having a triplet ground state,

$^3\Sigma$) will not relax the solvent protons during chromatographic experiments, increasing the ratio in $T_1$ between the long solvent $T_1$ and the short polymer $T_1$ further. A spoiler gradient is implemented at the end of the sequence to dephase the residual magnetization, as after a short $t_{rep}$, especially the solvent spins have not fully relaxed. Without this, strong residual solvent magnetization could cause baseline distortions [36].

In addition to these pulse sequence-based methods, post-acquisition methods can be applied solely or in combination with the solvent suppression methods mentioned. A simple and straightforward method of solvent suppression involves subtracting the solvent spectrum from a spectrum containing both the solvent and the analyte using a normal $^1$H pulse sequence (Fig. 1B, V) [34]. The limit of this method originates in the already mentioned final ADC digitization and the need for two separate measurements, and consequently, the drifts of the spectrometer between both measurements.

Another simple numerical post-acquisition suppression technique is the recently developed Solvent Attenuation by Fourier Elimination (SAFE) method within our group [37]. The principle involves recording spectra of both the pure solvent and the analyte solution under identical conditions, then applying Fourier transformation to reduce the solvent signal and average out drift contributions, substantially emphasizing the analyte signals. Multiple spectra are alternately acquired for each sample (e.g., via automatic sample exchange) and arranged in a 2D data matrix in an alternating sequence: 1. sample solution, 2. pure solvent, 3. sample solution, 4. pure solvent, and so on, for exactly $2^n$ times. This creates a periodic modulation of the analyte signals, see Fig. 2A. The 2D matrix starts with a spectrum of the PS sample, and the periodicity of the PS signals can be described by a zigzag function, shown in red in Fig. 2A. A fast Fourier transform (FFT) is then performed along the measurement series (i.e., over the time axis of the repeated measurements) at each data point along the chemical shift axis. For the simplest FFT, $2^n$ data points, respective spectra are needed. Periodically varying signals, such as those of the analyte, appear at the modulation frequency, $\nu_1$, in this case $\nu_1 = 0.21$ Hz,

$$\nu_1 = \frac{1}{T} = \frac{1}{2 * t_m} \quad (1)$$

with $T$ representing the period and $t_m$ the measurement time for one spectrum (with four scans used here $t_m = 2.4$ s). Constant signals (e.g. the solvent signal is approximately constant) appear at the zero frequency, $\nu_0$, while irregular or random signals are distributed across the frequency domain, see Fig. 2B. The $\nu_1$ frequency is analogous to the Nyquist frequency, which is the highest frequency that can be correctly represented in the frequency domain, as the periodicity is determined by sampling every second spectrum (with and without analyte). The spectrum at the highest frequency is then extracted and used for further data evaluation (see Section 4.1).

SAFE is particularly useful when common pulse-sequence-based solvent suppression methods are ineffective, for example, when there is strong overlap between the analyte and the solvent.

The post-acquisition methods can also be used in combination with other solvent suppression methods if an additional reduction of the residual solvent signal is required. Unlike simple solvent subtraction, SAFE considers changes in the spectra over time, like temperature fluctuations, drifts in chemical shift, and shimming values, to suppress constant solvent signals robustly. The spectra could also be recorded in a non-alternating way, with the alternation of data points applied after acquisition. However, in this case, periodicity or drift cannot be represented as accurately. When the spectra are alternated mechanically, changes due to temperature or field fluctuations affect both samples equally and cancel each other out at the modulation frequency. If, on the other hand, the alternation is generated "artificially" retrospectively, the data sets for the two states originate from different points in time. Meanwhile, signal intensities, line widths, and chemical shifts may have changed slightly. Such deviations are not constant and therefore wouldn't be suppressed efficiently by this method. The disadvantage is that SAFE cannot easily be implemented in continuous flow set-ups.

## 3. Materials and methods

### 3.1. Materials

Anionically polymerized, monodisperse PS samples with molecular weights of 1, 12, 125, 271, 552, 864 kg·mol$^{-1}$ (abbreviated as 1k, 12k, 125k, 271k, 552k, and 864k in the following) were purchased from the former Polymer Standards Service, PSS (now Agilent Technologies, Waldbronn, Germany). Of each sample, 2.5 g·L$^{-1}$ were dissolved in tetrahydrofuran (THF, GPC grade with 0.025 % butylated hydroxytoluene (BHT), Thermo Fisher Scientific, USA), chloroform ($CHCl_3$, GPC grade stabilized with 0.01 % Amylene, Thermo Fisher Scientific, USA) or deuterated chloroform ($CDCl_3$, 99.8 % with 1 v/v % TMS, Thermo Fisher Scientific, USA) and transferred into a 5 mm standard NMR tube (Deutero GmbH, Kastellaun, Germany) for static NMR measurements.

### 3.2. Methods

All NMR experiments were performed on a Spinsolve 90 Carbon ULTRA benchtop NMR spectrometer (Magritek, Aachen, Germany) running at a $^1$H Larmor frequency of 90 MHz, corresponding to a magnetic field strength of 2.1 T The permanent magnet is built in a Halbach design with a horizontally oriented magnetic field [38]. The spectrometer is equipped with a gradient coil with a maximum gradient strength of 0.53 T·m$^{-1}$ operating along the transverse plane. Linewidths for 20 % $CHCl_3$ in deuterated acetone are $< 0.2$ Hz at FWHM, $< 8$ Hz at 0.55 %, and $< 16$ Hz at 0.11 % peak height, according to the manufacturer's specifications. The magnet temperature was set by Magritek to 26.5 °C, and the samples for static NMR measurements were equilibrated in the magnet for five minutes before detection to avoid line broadening due to disturbed thermal equilibrium of the NMR and thermal convection inside the sample. Spectra were recorded and pulse sequences were modified using the SpinsolveExpert software (version 2.02.14).

Parameters for static NMR measurements were optimized for all solvent suppression methods under different aspects to achieve the best possible solvent suppression, as explained in more detail in Sections 3.2.1 to 3.2.9. This suppression efficiency was evaluated and quantified using the Analyte-to-Solvent Ratio (ASR) which is the ratio of the signal, $S$, of the aromatic $m/p$-protons of PS at 7.1 ppm to the intensity of THF at 3.6 ppm, $ASR = S_{Analyte}/S_{Solvent}$.

After method optimization, each method was repeated ten times to analyze repeatability. To test the methods' intermediate precision, all samples were prepared and measured on two different days. Four scans with 4096 data points and a dwell time of 100 µs, resulting in an acquisition time of 0.41 s per scan, were taken for each measurement for all methods. For data evaluation of NMR measurements, Mestrelab Mnova (14.1.2) was used. NMR spectra were zero and first order phase corrected, zero-filled to 64k data points, and the FID multiplied with a Gaussian apodization filter with a standard deviation, $\sigma$, of 0.47 s. This value was found to be optimum for polymer samples as the best compromise between high resolution and improved SNR. Baseline correction was done using a 3rd order polynomial. An overview of the pulse sequences used here is given in Fig. 1B, I-V and Sections 3.21 to 3.2.9.

#### 3.2.1. $^1$H reference, no suppression

Pulse length for 90° pulse was 13.7 µs with an amplitude of 0.0 dB, $t_{rep}$ was 0.6 s. The method was optimized to a maximum RG of 19–28 dB, see supporting information (SI) Fig. SI 1. Unsuppressed reference NMR spectra of PS in THF, $CHCl_3$, or $CDCl_3$ are shown in Fig. 1A, Section 2.

#### 3.2.2. PRESAT

The "PRESAT multi" sequence integrated into the SpinsolveExpert software was used to suppress the signals of THF at 3.6 ppm and 1.8 ppm. During optimization, the duration of the soft pulse was first varied from 0.5 to 5.0 s. It was found that the best ASR was achieved with a pulse duration of 1.5 s (see Fig. SI 2). The soft pulse amplitude was then varied from −85 dB to −25 dB, keeping the soft pulse duration at 1.5 s, with an optimum ASR for −55 dB. The receiver gain, RG, was optimized within the 10–64 dB range. A plateau in the Signal-to-Noise Ratio, SNR, was observed between RG = 28 and 64 dB (see Fig. SI 2). Higher RG values caused signal distortions due to FID clipping, while an RG of 10 dB led to insufficient intensity digitization, resulting in poor SNR for the analyte peaks. The hard pulse was set to a default length of 39.8 μs and an amplitude of −9.9 dB for a 90° pulse, or 0.0 dB for every second 270° pulse. Subtracting the two data sets afterwards further suppresses residual water signals [39]. The spoil amplitude was set to 10,000 (arbitrary software unit) with a duration of 20 ms, corresponding to ~18 $mT \cdot m^{-1}$. The $t_{rep}$ for PRESAT under these conditions was 2.2 s.

#### 3.2.3. WET

The default amplitudes for the four soft pulses are −67, −65, −68, and −61 dB, which is similar to varying the initial amplitude of −66 dB in steps of −1, +1, −2, and +5 with a pulse length of 86 ms for each pulse. The spoiler gradient pulses, each lasting 20 ms and starting at 20,000 a.u. (~40 $mT \cdot m^{-1}$), decrease by half for each spoil pulse (in total four) to dephase residual coherences in all spatial dimensions and systematically compensate for errors in $B_1$ [23,40].

Here, both the pulse length and amplitude of the soft pulses were optimized (see Fig. SI 3). It was found that a pulse length of 50 ms with an initial amplitude of −55 dB, resulting in values of −56, −54, −57, and −50 dB for the four pulses, yielded the best results. The length of the 90° pulse was set by default to 120 μs, with an amplitude of −18.7 dB. The RG yielded an optimum for 37 dB (see Fig. SI 3). The shortest possible $t_{rep}$ under these conditions was 1.0 s.

#### 3.2.4. PGSTE

The gradient duration ($\delta$) and gradient strength ($g$) were first optimized for PS12k. This molecular weight was chosen to optimize the method for polymers above 10 $kg \cdot mol^{-1}$, a molecular weight range relevant for most polymer chemists in academia and industry. For method optimization, it was specified that the weaker aliphatic peaks, appearing as a broad signal from 0.8 to 1.8 ppm, should remain above the limit of detection (SNR > 3). A Δ of 20 ms was used, which corresponds to the minimum possible delay time of the pulse sequence and minimizes signal losses due to $T_1$ relaxation. A range of 1–5 ms was investigated for $\delta$. The duration of 3 ms was found to be optimal (see Fig. SI 4). Shorter times led to reduced suppression of the solvent signal, while $\delta$ of > 3 ms already resulted in significant attenuation of the analyte signal. Then $g$ was varied at a constant $\delta$ of 3 ms, starting from 10 % (0.05 $T \cdot m^{-1}$) of the maximum available $g$ and increasing to 98 % (0.52 $T \cdot m^{-1}$). The $g$ was kept below 100 % to avoid damaging the gradient coils. The best ASR was achieved at 98 % (see Fig. SI 4). Additionally, a spoiler gradient of 5 ms with an amplitude of 5000 a.u., corresponding to ~9 $mT \cdot m^{-1}$, is implemented after the second 90° pulse to remove the residual transverse magnetization to prevent undesirable echo signals [41]. The length of the 90° pulse was set by default to 120 μs, with an amplitude of −18.7 dB. An RG of 46 dB was chosen for all measurements, see Fig. SI 4. The minimal possible $t_{rep}$ for PGSTE measurements resulted in 1.25 s. To measure the diffusion coefficient, $D$, of THF (resulting in $D = 2.19 \times 10^{-9}$ $m^2 \cdot s^{-1}$), the following parameters were used: $\delta = 5$ ms, $\Delta = 300$ ms, and 32 logarithmically spaced gradient steps ranging from 7 $mT \cdot m^{-1}$ to 70 $mT \cdot m^{-1}$, each with 8 scans, and a $t_{rep}$ of 3 s. All other parameters were kept the same.

#### 3.2.5. 1-Pulse-spoil

The method was optimized for different $t_{rep}$ of 0.5 to 2.5 s. Fig. SI 5 shows that shorter $t_{rep}$ increases solvent suppression efficiency, as more solvent magnetization remains unrelaxed. Therefore, a minimum $t_{rep}$ of 0.5 s was selected. Achieving such short measurement times was possible by adjusting the pulse sequence with a loop function in previous work by our group [17,36], which reduced data transfer and storage delays. Consequently, the 1-pulse-spoil sequence is faster than the regular $^1H$ sequence without suppression (0.6 s). The spoiler gradient was set to 10 ms duration with an amplitude of 5000 a.u., corresponding to ~9 $mT \cdot m^{-1}$. The pulse length for the 90° pulse was 13.7 μs with an amplitude of 0 dB. The optimal RG was between 19 to 37 dB, see Fig. SI 5.

#### 3.2.6. Simple solvent subtraction

Spectra containing diluted samples or the respective pure solvent (THF or $CHCl_3$) were recorded under the same conditions as the reference spectrum without suppression (see Section 3.2.1). For data evaluation, all spectra were first referenced to the same frequency at the solvent peak intensity of 3.6 ppm (for THF samples) or 7.2 ppm (for $CHCl_3$ samples). The solvent peak intensity at this frequency was then normalized to the same intensities for all spectra, after which the spectra of the pure solvent were subtracted from the sample spectra containing the same solvent. This was kept as simple as possible ("simple solvent subtraction") to ensure automated data processing for SEC—NMR measurements. Further method development could be explored in future investigations, e.g., by individually scaling the reference spectra before subtraction.

#### 3.2.7. SAFE

Similarly to solvent subtraction, the spectra were recorded under the same conditions as the reference spectrum without suppression (see Section 3.2.1). Samples (pure solvent and solvent with PS) were measured 16 times in total (8 of each), with measurements in alternating order to allow for FFT afterwards, see Fig. 2. To investigate the influence of the number of data points on suppression efficiency, $2^n$ spectra with n = 1, 2, 3, and 4 were recorded. For the case of two spectra, these were stacked eight times after acquisition to obtain a dataset with 16 spectra before Fourier transformation. The residual solvent intensity decreased slightly with more data points (see Fig. SI 6). Thus, 16 spectra were chosen as the optimal condition for SAFE solvent suppression. Recording >16 spectra was not pursued, as this would have considerably increased the total measurement time. Artificially repeating the 16-spectra dataset four times (64 points in total) yielded no further enhancement in solvent suppression, indicating that no improvement is obtained by artificially increasing the spectral resolution along the axis of the stacked spectra, as no new information is obtained.

#### 3.2.8. Longitudinal relaxation time $T_1$

Apparent longitudinal relaxation times ($T^*_1$) for the aromatic protons of PS (from 0.7 s for 1k to 0.4 s for 864k) were determined with an inversion recovery experiment with 20 spectra, 16 scans per spectrum, a repetition time of 5 s, and a maximum delay time, $\tau$, of 2.5 s. Pulse length for 90° pulse was 13.7 μs with an amplitude of 0 dB.

#### 3.2.9. SEC—NMR

SEC—NMR measurements were conducted using an SEC system (Agilent 1260 Infinity series), equipped with an isocratic pump, degasser, autosampler, fraction collector, as well as a UV and refractive index detector. WinGPC software (version 1.1, build 11,492, Agilent Technologies) was used for controlling the pump, as well as for data acquisition with the UV detector at 254 nm irradiation.

THF was used as a solvent and mobile phase at 1 mL $min^{-1}$. 500 μL of a bimodal sample mixture of PS12k and PS271k, each concentrated at 2.5 $g \cdot L^{-1}$ was injected into a semipreparative column (SDV linear M, 300 × 20 mm i.d., 10 μM particle size, mixed bed) obtained from PSS/Agilent. The column oven (SECurity$^2$, TCC6500) was set to 26.5 °C, similar to the NMR magnet temperature, to reduce drifts in chemical shift due to

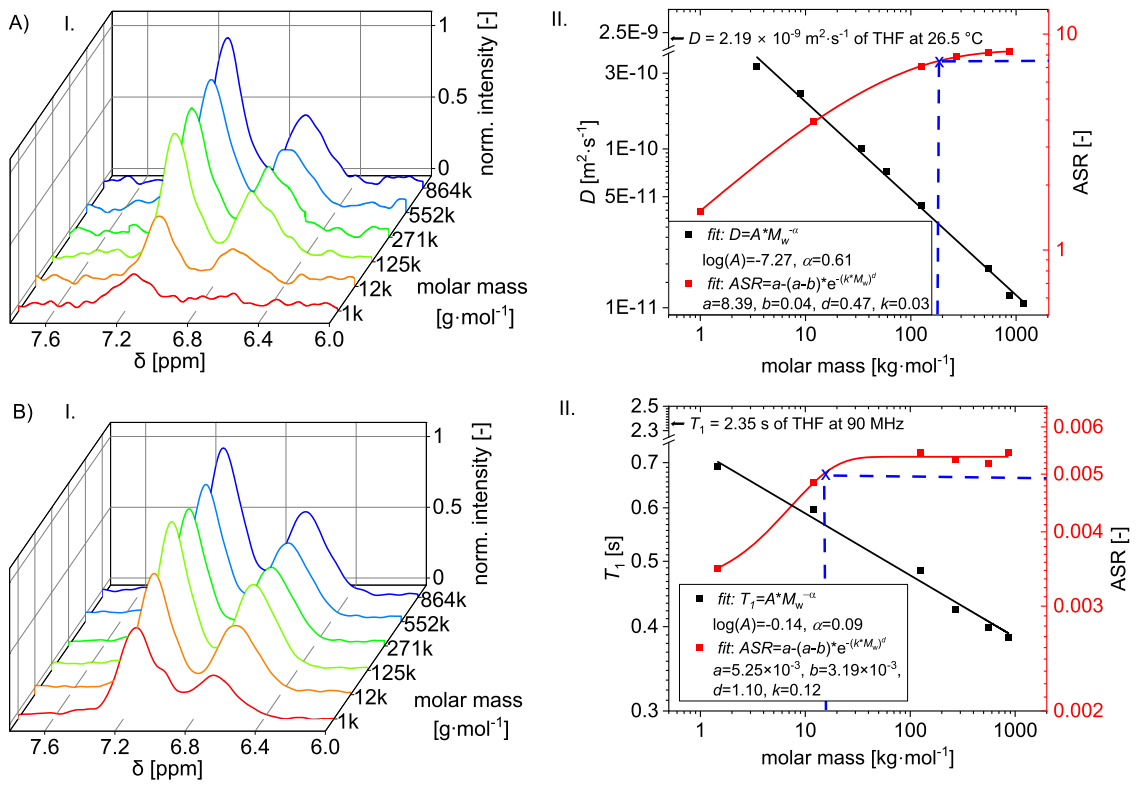


**Fig. 3.** Dependence of PS molar masses (1 to 864 kg·mol$^{-1}$) on PGSTE A) and B) 1-pulse-spoil solvent suppression efficiency. (A) Dependence of the diffusion coefficient ($D$) and the analyte-to-solvent ratio, ASR, of the PGSTE sequence (with a gradient duration of 3 ms and a gradient strength of 98 % (0.52 T·m$^{-1}$)) as a function of molar mass. ASR increases with higher molar masses. 90 % of the maximum ASR is reached at ~190 kg·mol$^{-1}$ (indicated by the blue dotted lines). With higher molar masses no significant signal reduction of the analyte is observed, with the ratio between solvent and analyte in $D$ being greater than two orders of magnitude. (B) Dependence of ASR on longitudinal relaxation times ($T_1$) and on molar masses for the 1-pulse-spoil pulse sequence. At molar masses > 15 kg·mol$^{-1}$, 90 % of the maximum ASR is reached, indicated by the blue dotted lines. Above this point, the $T_1$ ratio between solvent and analyte is greater than 4.

differences between magnet and solvent temperature. A custom-built glass flow cell with an active volume of 211 µL and a total volume of 496 µL was used for coupling to the NMR spectrometer, similarly to previous work in SEC—NMR at 62 MHz [36]; for detailed information of the SEC—NMR setup, the reader is referred to the Ph.D. thesis of Dr. Carlo Botha and publication of Botha et al. [36,42]. A picture and a schematic illustration of the current SEC—NMR setup can be found in Fig. SI 7. The spectra were acquired consecutively with 16 scans per spectrum during chromatographic separation with WET or PGSTE sequence, or a combination of both methods. All other NMR parameters were kept the same for WET and PGSTE pulse sequences as optimized under static conditions.

For each spectral point, the NMR intensities along the SEC dimension were smoothed by convolution with a Gaussian function, with a standard deviation $\sigma = 32$ s in WET and $\sigma = 40$ s in PGSTE experiments. To further enhance sensitivity, projections of NMR spectra are obtained by averaging across the FWHM of the 2D peaks in the $y$-dimension (elution time, min), and NMR "chromatograms" are obtained by averaging across the FWHM of the 2D peaks in the $x$-dimension (chemical shift, ppm) [37]. The contour plots were generated using eight logarithmically spaced intensity levels ranging from $4\sigma$ to $500\sigma$ of the noise intensity from 5.0 to 5.5 ppm.

## 4. Results and discussion

### 4.1. Solvent suppression under static NMR conditions

PS standards were dissolved in THF or $CHCl_3$. The effectiveness of the solvent suppression methods was evaluated based on the following criteria: (1) molar mass dependency on the ASR, (2) reduction of the solvent peak signal and selectivity, i.e. suppression of neighboring analyte peaks, under optimized method parameters, (3) repeatability and intermediate precision, i.e., relative standard deviation of the ASR values (coefficients of variation, CVs), and (4) measurement time efficiency by evaluating the minimum possible duration of each experiment for optimized suppression.

#### 4.1.1. Molar mass dependency

The suppression efficiency of frequency-selective methods, such as PRESAT and WET, depends on the signal's linewidth. Suppressing solvent molecules may also result in the partial attenuation of broad resonances of macromolecules that overlap with the solvent. Smaller analyte molecules typically show narrower linewidths, making them less likely to be obscured by nearby solvent molecules. This frequency dependency does not apply to the other four suppression methods. However, diffusion- and $T_1$-based methods such as PGSTE and 1-pulse-spoil exhibit a much stronger molar mass dependency due to the following other effects:

PGSTE achieves efficient solvent suppression when the analyte has a significantly lower diffusion coefficient $D$ than the small solvent molecules, making it particularly effective for macromolecules. The suppression efficiency was tested for the PS standards, ranging from 1 to 860 kg·mol$^{-1}$. Fig. 3A shows that no further suppression of the analyte signals was observed when the previously optimized PGSTE parameters were applied to PS samples with molar masses above 190 kg·mol$^{-1}$. The reduction of the maximum ASR for higher molar masses is < 10 %, based on a fit using a Weibull-like function that exhibits exponential growth followed by saturation, see Fig. 3A, II. The point of 10 % deviation from the maximum ASR is marked with a blue cross. The diffusion coefficient $D$ of PS samples with different molar masses, together with $D$ of THF at

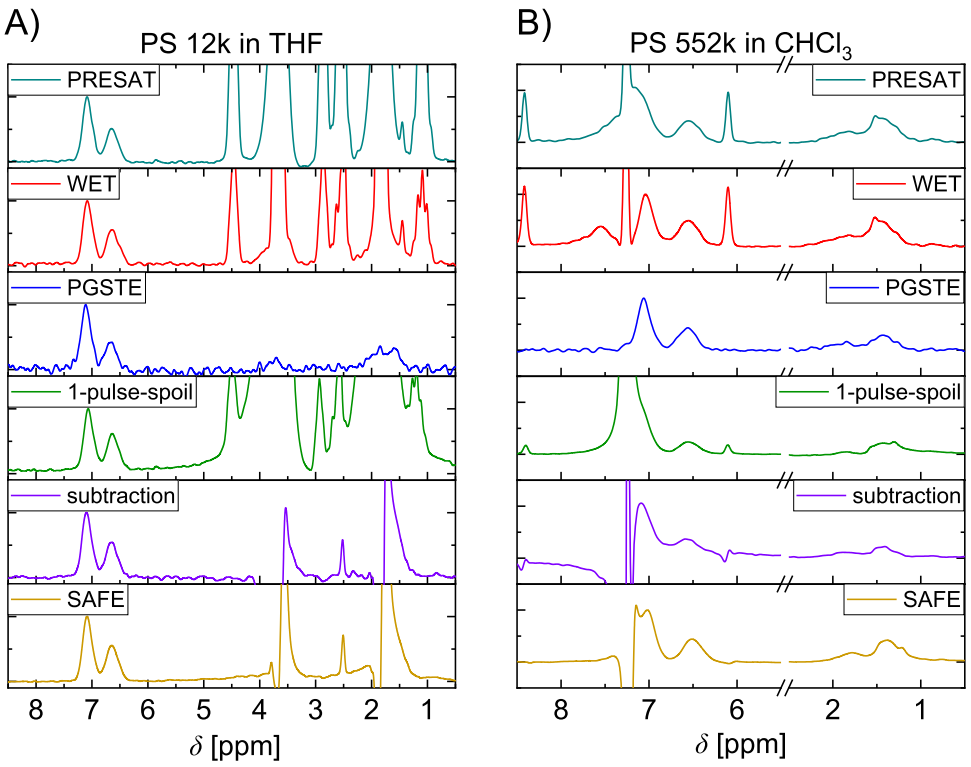


**Fig. 4.** Overview of NMR spectra of all solvent suppression methods after optimization. (A) 12 kg·mol$^{-1}$ Polystyrene (PS) in THF. (B) 552 kg·mol$^{-1}$ PS in $CHCl_3$. The following suppression methods were applied (from top to bottom): Presaturation (PRESAT), Water suppression enhanced through $T_1$ effects (WET), Pulsed gradient stimulated echo (PGSTE), 1-pulse-spoil, mathematical solvent subtraction, and solvent attenuation by Fourier elimination (SAFE). All spectra are normalized to the intensity of the aromatic *m/p*-protons of PS at 7.1 ppm. For experiment parameters and evaluation, see Section 4.1.2 and Table 1 in Section 4.1.4.

26.5 °C, are plotted in the graph as well, where data for PS samples were taken from Tratz et al. [43], $D$ of THF was measured and calculated as described in Section 3.2.4 and Fig. SI 8. The results show that a $D$ ratio of almost two orders of magnitude ($2.19 \times 10^{-9}$ m$^2$·s$^{-1}$ for THF versus $\sim 3.54 \times 10^{-11}$ m$^2$·s$^{-1}$ for PS with a molar mass of 190 kg·mol$^{-1}$) is required to prevent attenuation of the analyte signal. If the focus of the analysis is on polymers with molar masses below 190 kg·mol$^{-1}$, it should be considered whether a reduction in the analyte signal can be tolerated, e.g., if the samples are highly concentrated. Otherwise, $g$ or $\delta$ must be minimized, and a lower ASR has to be accepted.

As the 1-pulse-spoil method relies on the $T_1$ difference between the analyte and the solvent, and $T_1$ varies with molar mass (see Fig. 3B), the ASR dependency was tested using the same PS samples as for the PGSTE method. Fig. 3B shows that the ASR is worse for molar masses lower than 15 kg·mol$^{-1}$, with an ASR that is > 10 % smaller than the maximum ASR, indicated by the blue cross. A nearly constant ASR is reached above this value. The partial suppression of molar masses below 15 kg·mol$^{-1}$ results from a rather similar $T_1$ between analyte ($T_1$ greater than 0.6 s) and solvent ($T_1 = 2.35$ s). Above a $T_1$ ratio of greater than 4, however, only the solvent is suppressed for the given repetition time [36].

### 4.1.2. *Suppression efficiency*

The performance of the suppression methods in THF (A) and $CHCl_3$ (B) is summarized in Fig. 4A and B. The suppression efficiency was quantified by the Analyte-to-Solvent Ratio normalized to the ASR reference without any suppression technique applied, $ASR_{norm}$. The reference spectrum of PS in THF or $CHCl_3$ without solvent suppression is shown in Fig. 1A.

With PRESAT, the aromatic protons of PS12k at 6.3–7.3 ppm were separated from THF, while the aliphatic region around 1.5 ppm still overlapped with the remaining solvent peaks. As no Carbon-decoupling element was applied, the $^{13}$C satellites remained visible in the PRESAT spectrum. Under optimized conditions, an $ASR_{norm}$ of 143 was obtained for PRESAT, with the efficiency depending strongly on $B_0$-field homogeneity. In $CHCl_3$, PRESAT similarly reduced the intensity and width of the solvent resonance, making the aromatic *m/p*-protons of PS552k detectable, though partial overlap persisted. WET provided an $ASR_{norm}$ of 115 for PS12k in THF, quite similar to PRESAT, but with narrower residual solvent peaks (FWHM of 11.1 Hz vs. 16.0 Hz for PRESAT). For PS 552k in $CHCl_3$, WET likewise offered better selectivity, with aromatic protons more clearly resolved.

PGSTE achieved the most effective suppression, with an $ASR_{norm}$ of 7619 for PS12k in THF and nearly complete removal of the chloroform resonance of PS552k in $CHCl_3$. Aromatic and aliphatic signals were clearly visible in both solvents, and $^{13}$C satellites were eliminated without the need for decoupling since it is a non-frequency-selective method. Although the analyte signal intensity was also reduced due to a difference in $D$s of only one order of magnitude between solvent and analyte for PS12k (see Fig. 3A), PGSTE has the advantage of being non-frequency-selective, making suppression independent of resonance frequencies and $B_0$-field homogeneity. The 1-pulse-spoil method yielded only limited suppression efficiency with $ASR_{norm} = 7$ for PS12k in THF and residual spectral feet remaining broad (~230 Hz), obscuring aliphatic PS signals. In $CHCl_3$, a strong overlap between analyte and solvent could still be observed, thus, a combination of 1-pulse-spoil with post-acquisition solvent suppression is essential [17,36].

Among post-acquisition methods, simple solvent subtraction achieved an $ASR_{norm}$ of 278, effectively removing $^{13}$C satellites while leaving residual solvent peaks with partially negative intensities. To remove such artefacts, further method optimization could be investigated in future work, e.g., by adaptively scaling the reference spectra before subtraction. The broader THF peak at 1.8 ppm compared to the THF peak at 3.6 ppm indicates aliphatic contributions from PS beneath the solvent resonance. In $CHCl_3$, subtraction likewise reduced the solvent resonance with remaining negative artifacts. The spectrum obtained with SAFE resembles the solvent-subtracted spectrum but has an

**Table 1**
Overview of the properties of all suppression methods examined after optimization of 2.5 $gL^{-1}$ PS12k in THF. The SNR (signal-to-noise ratio) values of the PS intensities at 7.1 ppm are normalized to the square root of measurement time (4 scans). The ASR (analyte-to-solvent ratio) values are normalized to the ASR value of the unsuppressed reference spectrum.

| Parameter | no supp. | PRESAT | WET | PGSTE | 1-pulse-spoil | subtraction | SAFE | PGSTE+SAFE |
|---|---|---|---|---|---|---|---|---|
| Experiment duration (1 scan) [s] | 0.6 s | 2.2 s | 1.0 s | 1.25 s | 0.5 s | 0.6 s*2 = 1.2 s | 0.6 s*16 = 9.6 s | 1.25 s * 16 = 20 s |
| SNR/$\sqrt{t}$ [1/$\sqrt{s}$] (at 7.1 ppm) | 48 | 30 | 38 | 14 | 50 | 28 | 29 | 15 |
| $ASR_{norm}$ [-] | 1 | 143 | 115 | 7619 | 7 | 278 | 584 | 47,143 |
| $CV_{Repeatability}$ (10x measured) | 2.11 % | 6.94 % | 1.26 % | 7.24 % | 3.24 % | 32.5 % | 4.39 % | - |
| $CV_{Precision}$ (2x, 2 days, 2 samples) | 5.23 % | 15.2 % | 2.47 % | 9.00 % | 4.91 % | 65.0 % | 31.1 % | - |
| Suitable for small molecules | - | yes | yes | no | no | yes | yes | no |

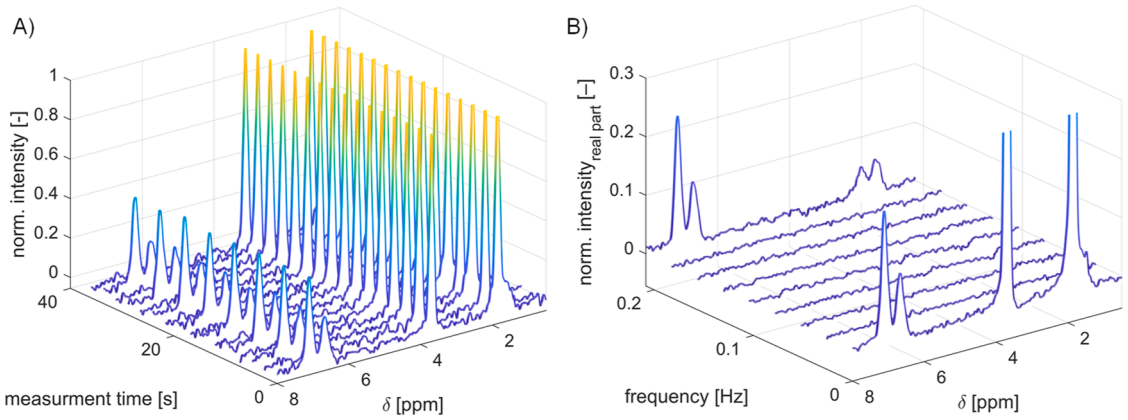


**Fig. 5.** Combination of PGSTE and SAFE solvent suppression methods. (A) Periodic arrangement of pure THF and sample (PS12k) dissolved in THF after PGSTE solvent suppression with 75 % gradient strength. (B) FT at each chemical shift leads to the solvent-filtered Fourier spectrum. Only the real parts are shown. The spectrum at the modulation frequency (0.21 Hz, last spectrum) is the resulting solvent-suppressed spectrum with an $ASR_{norm}$ of 47,140. Spectra are normalized to the maximum solvent peak intensity at 3.6 ppm.

improved $ASR_{norm}$ of 584.

To effectively suppress constant components for both solvent subtraction and SAFE, samples should be measured under identical conditions (shim, temperature, and field homogeneity). Slight differences in chemical shift or line shape, caused by variations in these factors, reduce suppression efficiency and can introduce artefacts into the spectrum. See Section 4.1.3, "Repeatability and intermediate precision", for a more detailed discussion. All $ASR_{norm}$ values are summarized in Table 1.

Overall, the PGSTE produced by far the best $ASR_{norm}$ results for PS samples in comparison to the other methods. While this method has the disadvantage of partially reducing the analyte signals for lower molar mass polymers, it could be applied with weaker gradient strengths to preserve the analyte signals better. As solvent signals are not fully suppressed under weaker gradient conditions, a combination of post-acquisition methods could therefore be useful. Fig. 5 shows the results of combining PGSTE, with 75 % gradient strength (ca. 0.375 T/m) and keeping the other PGSTE parameters constant, with the SAFE method. Without SAFE, the aliphatic protons are still overlaid by residual THF signals at 75 % gradient strength (see Fig. 5A or the spectrum at $\nu_0$ in Fig. 5B). After FFT along the stacked spectra, the solvent signals are almost completely suppressed (see spectrum at $\nu_1$, last spectrum in Fig. 5B), and an $ASR_{norm}$ of 47,140 could be achieved, which is a further ~6-fold improvement in $ASR_{norm}$ compared to PGSTE alone at 98 % gradient strength, as the analytes are not suppressed as much. Therefore, combining PGSTE with a weaker gradient strength alongside SAFE is recommended to preserve the signal of the analytes more effectively and suppress the solvent more effectively for polymers. Additionally, the effect of a PGSTE gradient strength of 50 % in combination with SAFE was tested. This resulted in better solvent peak suppression than without SAFE, although the $ASR_{norm}$ was 7,558, which is worse than at 75 % gradient strength (see Fig. SI 9).

#### 4.1.3. *Repeatability and intermediate precision*

To assess repeatability, each suppression method was repeated ten times, and intermediate precision was further tested by preparing and measuring samples on two different days. ASRs (Analyte-to-Solvent Ratios) were used for the calculation of the CVs (Coefficient of Variation). All data are summarized in Table 1. For PRESAT, CVs were 4.96 % for repeatability and 15.2 % for intermediate precision, strongly depending on the $B_0$-field homogeneity. WET performed best with CVs of 1.26 % and 2.47 %. PGSTE showed CVs of 7.24 % and 9.00 % for repeatability and intermediate precision, respectively, indicating reliability similar to that of PRESAT, but lower than that of WET. The 1-pulse-spoil experiments gave CVs for repeatability and intermediate precision of 3.24 % and 4.91 %, respectively. Solvent subtraction performed poorly in comparison to the other methods, with CVs of 32.5 % and 65.0 %. Such poor performance arises because solvent subtraction is done manually and is highly sensitive to small inconsistencies, magnetic field drifts, shimming variations, phasing, and sample contaminations [44]. Furthermore, minor differences in line shapes or chemical shifts can result in subtraction artefacts, such as negative peaks. These artefacts cause significant fluctuations in the signal intensity of the remaining solvent signals. While the solvent subtraction can be combined with other suppression techniques to enhance efficiency without additional expense or method development, it should be considered that manual solvent suppression may compromise the repeatability and

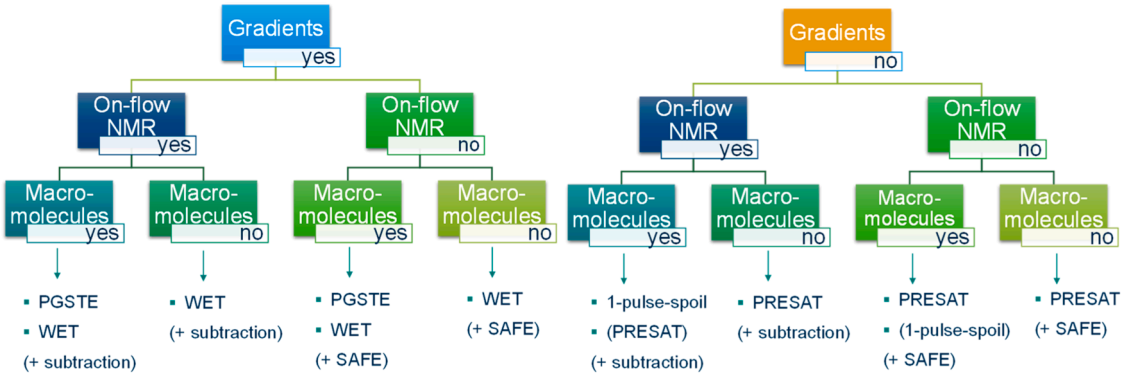


**Fig. 6.** Flow chart of which solvent suppression method investigated here is most suitable for the given experimental requirements, such as the availability of magnetic field gradients and the need for short measurement times, e.g., on-flow reaction monitoring or HPLC—NMR, as well as whether macromolecules will be analyzed. Post-acquisition suppression methods are placed in brackets as they can be used in combination with the other pulse sequence-based suppression methods.

precision of the experiment. By contrast, the SAFE method was found to be more reliable than the subtraction method, with CVs of 4.39 % and 31.1 % for repeatability and intermediate precision, respectively. The critical aspects of reliable solvent subtraction discussed previously for the subtraction method also apply to the SAFE method. Better reliability could be achieved since 16 spectra were recorded for SAFE, enabling fluctuations or drifts to be averaged out more effectively. In contrast, only two spectra were used for the simple solvent subtraction method. Furthermore, temporal changes in the spectra have less impact on SAFE, as the periodicity of the alternating measurements can compensate for them more effectively, and the FFT is more robust compared to manual subtraction.

#### 4.1.4. Time efficiency

Although increasing the saturation pulse duration improves the selectivity of the PRESAT pulse, this also increases the overall experiment time. This is particularly disadvantageous when coupled with chromatography or on-flow reaction monitoring because the spins are usually only in the active region of the NMR coil for a few seconds. WET and PGSTE sequences are advantageous here, as they achieve shorter $t_{rep}$ (min. 1.0 s or 1.25 s per scan, respectively) compared to PRESAT with 2.2 s per scan under the optimized conditions (see Section 3.2). Comparing the SNR values of the PS12k signal at 7.1 ppm normalized to the square root measurement time (SNR/$\sqrt{t}$), WET gives better results (= 38/$\sqrt{s}$) than PGSTE (= 14/$\sqrt{s}$). This low SNR/$\sqrt{t}$ value is the main drawback of PGSTE, particularly at molar masses below 190 kg·mol$^{-1}$ (see Section 4.1.1, "Molar Mass Dependency", for a detailed discussion), as it suppresses the solvent signal as well as partially analyte signals. Although the 1-pulse-spoil sequence is significantly less efficient in terms of solvent suppression, its short $t_{rep}$ of 0.5 s per scan makes it ideal for on-flow measurements. With an SNR/$\sqrt{t}$ of 50/$\sqrt{s}$, 1-pulse-spoil performs best in comparison to all other methods. In combination with solvent subtraction, it still gives satisfactory results for solvent suppression in SEC—NMR measurements [17,36].

The total measurement time for SAFE is 9.6 s (with one scan per spectrum and 16 spectra, excluding the time for sample changes or the 5-min delay for temperature stabilization). Although with an SNR/$\sqrt{t}$ = 29/$\sqrt{s}$ the method gives similar results to solvent subtraction (= 28/$\sqrt{s}$), SAFE isn't suited to on-flow NMR applications as the samples need to be changed periodically.

Table 1 summarizes all previously discussed methods and their characteristics for NMR spectrometer with or without gradients. Depending on the sample type and experiment requirements, one method may be more suitable than another. Therefore, there is no single perfect solvent suppression method for all kinds of experiments. Fig. 6 shows a flowchart that guides which pulse sequences are most appropriate under various conditions, such as the availability of gradients in the spectrometer, the need for short measurement times when using HPLC—NMR or on-flow reaction monitoring, as well as whether macromolecules or small molecules are of interest. The solvent suppression methods available on the Spinsolve instruments from Magritek (except the 1-pulse-spoil sequence) are shown at the end of the diagram, which best fit the criteria selected in the flow chart. The post-acquisition methods SAFE and numerical solvent subtraction are also included in brackets, as these can always be combined with the proposed methods for more effective solvent suppression.

### 4.2. Application example for on-flow SEC-NMR with: WET, PGSTE and WET + PGSTE

An application example where solvent suppression for polymer solutions with protonated solvents is crucial is SEC—NMR [8,36,45,46]. When choosing the best solvent suppression method for SEC—NMR, it is important to consider that a fast method is required, since the analyte residence time in the active NMR region is only a few seconds as typical flow rates are 1 mL·min$^{-1}$ combined with a flow cell volume of 0.2 mL, leading to 12 s average residence time. Additionally, sample concentrations are even lower (typically 0.1 wt. % at peak maximum) compared to static NMR (e.g., 0.3 wt. %) to avoid column overloading and due to additional dilution during separation [9]. This makes solvent suppression methods particularly necessary to achieve sufficient sensitivity. The samples investigated with SEC are macromolecules, and since the 90 MHz spectrometer used for this setup is equipped with gradients up to 0.53 T·m$^{-1}$, PGSTE and WET can be applied as the most efficient and fastest methods (see the left path of Fig. 6). One challenge that arises when performing solvent suppression in on-flow NMR experiments is the so-called "faraway solvent" effect. Solvent molecules outside the central RF detection volume experience a weaker and less homogeneous RF field, making them more difficult to suppress, especially when the sample is flowing [47]. Further complications arise from frequency instabilities, which are common in on-flow NMR setups due to temperature fluctuations [48]. This issue is especially problematic in solvent-gradient-based LAC, where the eluent composition changes over time. These changes further exacerbate resonance drift, thereby reducing the efficiency of solvent suppression.

For SEC—NMR, a mixture of 2.5 g·mol$^{-1}$ of PS271k and PS12k was analyzed. 500 µL of the mixture was injected into a semi-preparative SEC column, corresponding to an injected mass of 1.25 mg of each polymer. This value was based on previous method development on SEC—NMR by this working group to achieve the maximum possible concentration for optimum NMR sensitivity while limiting SEC overloading [36]. The flow rate was set to 1 mL·min$^{-1}$, and a UV detector was used additionally after the NMR detector. For more detailed information on the on-flow NMR method, see Section 3.2.9, and literature [9,36]. For each NMR

spectrum, 16 scans were recorded and averaged, resulting in the PGSTE sequence recording one spectrum along the chromatogram every 20 s and the WET sequence recording one every 16 s. The other parameters

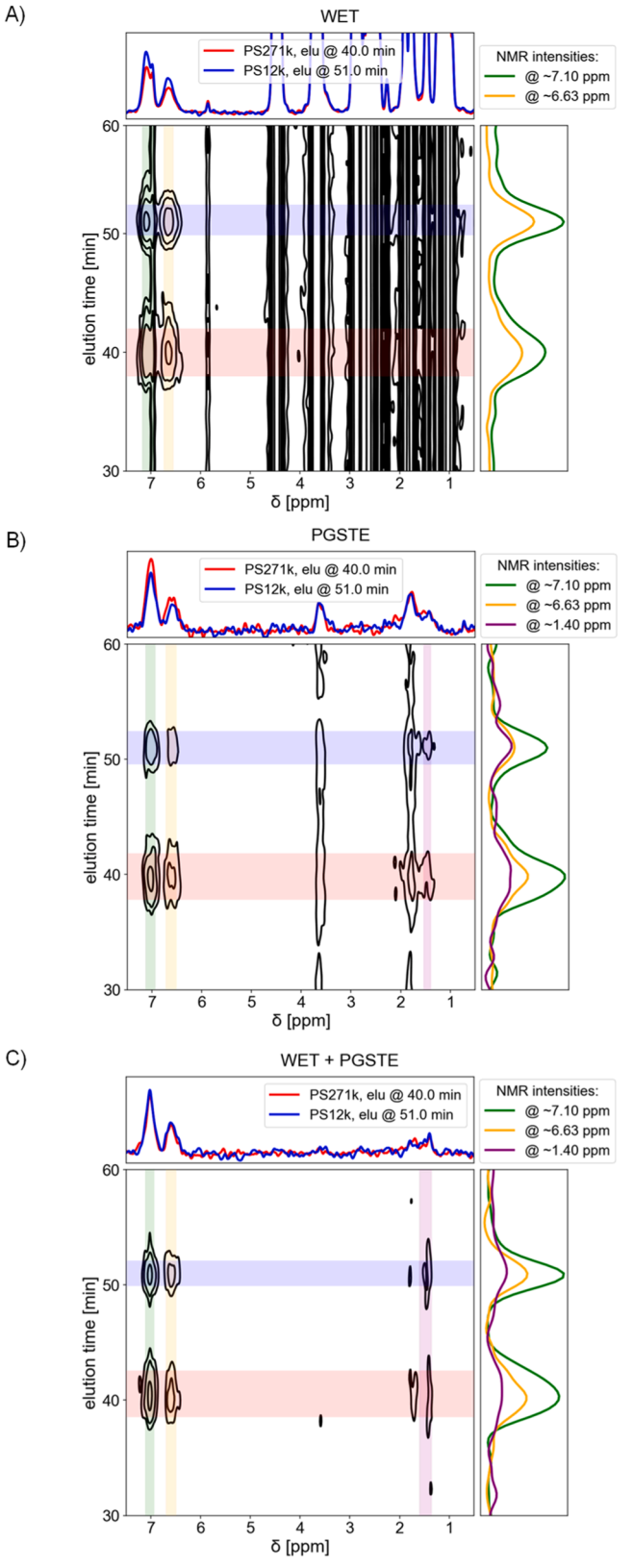


*(caption on next column)*

**Fig. 7.** SEC—NMR results of 2.5 $g{\cdot}L^{-1}$ PS12k and PS271k in THF at 1 $mL{\cdot}min^{-1}$. 2D contour plot with corresponding projections. (A) WET, (B) PGSTE (98 % gradient strength), and (C) WET and PGSTE (with a 75 % gradient strength) were used to suppress the solvent signal for each spectrum during the SEC—NMR run. The 2D plot for WET and mathematical solvent subtraction is shown in Fig. SI 11. The contour plots are plotted with 8 logarithmically spaced intensity lines ranging from four to 500 times the standard deviation of the noise intensity between 5.0 to 5.5 ppm. Projections of NMR spectra are obtained by averaging the intensities across the FWHM in the *y*-axis (elution time, min; top projections), NMR "chromatograms" are obtained by averaging the intensities across the FWHM in *x*-axis (chemical shift, ppm; right projections). The corresponding areas are highlighted in the 2D plot.

remained the same as those previously optimized and discussed in Section 3.2. Fig. 7 shows 2D plots of the spectral chromatogram as a contour plot. The projections of NMR spectra at the top of the 2D plot are obtained by averaging the signals across their FWHM in the *y*-axis (elution time, min). The NMR "chromatograms" at the right side of the 2D plot are obtained by averaging the peaks across their FWHM along the *x*-axis (chemical shift, ppm). The corresponding areas are highlighted in the 2D plot.

Fig. 7A and Table 2 show the results when WET is used as the method of choice. The remaining solvent signals are clearly visible as continuous lines throughout the 2D plot. The peaks at 1.4, 2.2, 5.9, and 7.0 ppm correspond to BHT, added as a stabilizer to THF. After 36 min, the higher molecular weight and consequently larger polymer (PS271k) elutes first, and the aromatic PS signals are clearly visible, with a maximum SNR of 36 at 7.11 ppm after 40 min of elution. Meanwhile, the aliphatic signals are still overlapped by the remaining solvent signals (THF SNR = 335 at 3.66 ppm). The second, lower molecular weight polymer in the sample, PS12k, elutes after 48 min, with its peak maximum at 7.11 ppm after 51 min. The resulting chromatographic peak is sharper and narrower than that of PS271k, resulting in increased NMR sensitivity of SNR = 43. Fig. SI 10 shows the UV chromatogram recorded at 254 nm for comparison to the "NMR chromatogram" based on NMR intensities. The resulting $ASR_{norm}$ after WET SEC—NMR was ~160. For better comparison to the PGSTE method, the results shown in Fig. 7A were not processed with additional mathematical solvent subtraction, as for PGSTE, no further post-acquisition solvent suppression is needed under the optimized conditions. Fig. SI 11 shows the combination of mathematical solvent subtraction with WET during an SEC—NMR measurement. Here, the spectra averaged over the signal-free region from 0 to 5 min of elution were subtracted from all other spectra in the SEC—NMR run. It is visible that the combined solvent suppression method is way more effective in reducing the remaining THF signal intensities ($ASR_{norm}$ ~600), although negative solvent peaks appear in the spectrum.

The PGSTE method (Fig. 7B) shows very weak remaining solvent signals (SNR = 7), and the weak BHT signals completely disappeared. As can be seen in the WET experiment and from the UV intensities (see Fig. SI 10), the chromatographic intensity of PS12k is higher than that of PS271k. However, in the PGSTE experiment, PS12k appears with slightly lower intensity than PS271k (PS271k SNR = 21 and PS12k SNR = 19), as stronger diffusion effects suppress the smaller-molar-mass polymer more. With an $ASR_{norm}$ of ~4000, the suppression efficiency is ~26x higher compared to the application of the WET sequence only.

As both methods have their benefits and drawbacks, a combination of WET and PGSTE, with weaker gradient strengths to preserve more analyte signal and increase SNR, especially for aliphatic protons, could be optimal. The combined pulse sequence contains the WET block before the PGSTE block, without the 90° hard readout pulse after the WET block. Instead, the magnetization is restored to the x-y plane for detection at the end of the PGSTE block. Different PGSTE gradient strengths, ranging from 25 % to 98 %, with a $\delta$ of 3 ms, were tested on the PS12k sample for the WET-PGSTE sequence, using the same WET parameters as those optimized in Section 3.1. Fig. SI 12 shows that, at a gradient strength of 75 %, the solvent peak is suppressed completely by a factor of

**Table 2**
The SNR and $ASR_{norm}$ values for SEC—NMR measurements of 2.5 g·L$^{-1}$ PS12k and PS271k with WET, WET combined with solvent subtraction, PGSTE with 98 % gradient strength (*g*), and the combination of WET and PGSTE with $g = 75$ % are shown. SNR was calculated at the peak maximum of elution (40 min for PS271k and 51 min for PS12k) for the aromatic protons of PS at 7.1 ppm and the THF peak at 3.7 ppm. $ASR_{norm}$ was calculated by normalizing to the ASR of each sample (PS12k and PS271k) from the unsuppressed SEC—NMR measurement.

| Method | Sample | SNR PS [-] | SNR THF [-] | $ASR_{norm}$ [-] |
|---|---|---|---|---|
| No suppression, reference | PS12k | 46 | 54 767 | 1 |
| | PS271k | 37 | 60 362 | 1 |
| WET | PS12k | 43 | 335 | 155 |
| | PS271k | 36 | 383 | 157 |
| WET + subtraction | PS12k | 44 | 84 | 624 |
| | PS271k | 33 | 94 | 585 |
| PGSTE, $g = 98$ % (0.52 T·m$^{-1}$) | PS12k | 19 | 7 | 3,231 |
| | PS271k | 21 | 7 | 5,000 |
| WET + PGSTE, $g = 75$ % (0.375 T·m$^{-1}$) | PS12k | 23 | 3 | 9,126 |
| | PS271k | 27 | 4 | 11,250 |

approximately $10^4$. Higher gradient strengths merely led to a further reduction of the analyte peak signal, while a gradient strength of 50 % could not completely suppress the solvent. For the following SEC—NMR measurements, the previously optimized WET parameters were used, along with a PGSTE gradient strength of 75 % instead of 98 %. Fig. 7C shows the result of the SEC—NMR measurement, revealing an almost complete reduction of the solvent signal. The aliphatic protons no longer overlap with the residual solvent peaks. For PS12k the SNR = 23, and for PS271k, SNR = 27. The solvent peak at 3.6 ppm is at the limit of detection (SNR ~3–4), with an $ASR_{norm}$ of ~10,000, making it easy to assign all peaks in the spectrum.

## 5. Conclusion

This work presents a systematic comparison of six solvent suppression methods, evaluated by the analyte-to-solvent ratio normalized to the ratio of the unsuppressed reference spectrum, $ASR_{norm}$. The study also considers the methods' repeatability and intermediate precision, applicability to small molecules and macromolecules, as well as measurement time, to ensure suitability for online NMR applications such as reaction monitoring or online HPLC—NMR. The investigated methods include PRESAT, WET, PGSTE, 1-pulse-spoil, solvent subtraction, and a novel post-acquisition technique we called Solvent Attenuation by Fourier Elimination (SAFE). SAFE alternates $2^n$-times between acquiring a sample containing analytes and solvent and acquiring a sample of pure solvent to introduce periodicity. Arranging the spectra in a two-dimensional data array effectively removes unperiodic signals through a second FFT while maintaining (filtering) the periodic modulated analyte signals.

PGSTE was shown to be the most efficient solvent suppression method for macromolecular samples. With an $ASR_{norm}$ of ~7,600 (for 2.5 g·L$^{-1}$ PS12k in THF) the method achieved the best results compared to all other single solvent suppression methods investigated here. Using PGSTE, Coefficients of Variation (CV) of 7 % for repeatability and 9 % for intermediate precision were achieved with a minimum measurement time of 1.25 s per scan. While this method can't be used for samples with small molar masses due to the insufficient difference (ratio) in diffusion coefficient, *D*, between analytes and solvent, WET proved to be the most effective method for samples containing small molecules. With WET, an $ASR_{norm}$ of 115, repeatability and intermediate precision of 1–2 %, and a measurement time of 1.0 s per scan could be achieved. In contrast, PRESAT ($ASR_{norm}$ of 143) suffers from lower selectivity than WET and longer measurement times due to long soft pulses. The 1-pulse-spoil method, used as a $T_1$-filter, is the fastest pulse sequence investigated here, with 0.5 s per scan, but is limited to macromolecules. Because solvent suppression can be insufficient with an $ASR_{norm}$ of 7 (for 2.5 g·L$^{-1}$ of PS12k), it should be combined with post-acquisition methods such as simple solvent subtraction or SAFE. Compared to simple solvent subtraction ($ASR_{norm}$ of 278), SAFE achieved a 2-fold better suppression ($ASR_{norm}$ of 584). Additionally, SAFE has a higher repeatability than the subtraction method (CV of 4 % versus 33 %). The main drawback of SAFE is the longer measurement time, as multiple spectra and exchange of samples are necessary, making it unsuitable for on-flow NMR. Furthermore, a combination of PGSTE (with reduced gradient strength) and SAFE was tested under static NMR conditions, resulting in an $ASR_{norm}$ of about 47,000 with nearly complete reduction of the THF solvent signals.

Finally, solvent suppression was applied to online SEC—NMR as a possible application example. The combination of WET and PGSTE was particularly effective, reaching an $ASR_{norm}$ of about 10,000. Even solvent resonances that fully overlap with analyte peaks could be eliminated, providing a significant advantage for the interpretation of complex spectra at a low-field spectrometer.

## CRediT authorship contribution statement

**Johanna Tratz:** Writing – original draft, Visualization, Software, Methodology, Investigation, Formal analysis, Data curation. **Markus Matz:** Writing – review & editing, Software, Methodology. **Manfred Wilhelm:** Writing – review & editing, Supervision, Funding acquisition, Conceptualization.

## Declaration of competing interest

The authors declare that they have no known competing financial interests or personal relationships that could have appeared to influence the work reported in this paper.

## Acknowledgments

The authors acknowledge financial support from Deutsche Forschungsgemeinschaft (DFG, grant WI 1911/35–1). The authors also thank Dr. B. Gizatullin (Magritek) for his helpful information on spectrometer details, as well as Dr. M. Gaborieau (KIT) and Dr. M. Pollard (KIT) for their overall support. Further, we would like to thank Prof. Dr. J. Brandner and KNMFi (www.knmf.kit.edu) for support towards the 90 MHz NMR spectrometer.

## Supplementary materials

Supplementary material associated with this article can be found, in the online version, at doi:10.1016/j.jmro.2025.100213.

## Data availability

Data will be made available on request.

## References

[1] K. Saalwächter, Applications of NMR in polymer characterization – an introduction, in: R. Zhang, T. Miyoshi, P. Sun (Eds.), NMR Methods for Characterization of Synthetic and Natural Polymers, The Royal Society of Chemistry, Cambridge, UK, 2019, pp. 1–22.
[2] T.D.W. Claridge, Chapter 12 - experimental methods, in: T.D.W. Claridge (Ed.), High-Resolution NMR Techniques in Organic Chemistry, Elsevier, Boston, 2016, pp. 457–496.
[3] S.B.S. Berger, 200 and More NMR Experiments: A Practical Course, 3rd ed, Wiley-VCH, Weinheim, Germany, 2005.
[4] P. Kilz, H. Pasch, Coupled liquid chromatographic techniques in molecular characterization, in: T. Provder, R.A. Meyers (Eds.), Encyclopedia of Analytical Chemistry: Applications, Theory and Instrumentation, John Wiley & Sons Ltd, Chichester, UK, 2000, pp. 495–7543.
[5] N. Watanabe, E. Niki, Direct-coupling of FT-NMR to high performance liquid chromatography, Proc. Jpn. Acad. Ser. B 54 (1978) 194–199, https://doi.org/10.2183/pjab.54.194.

[6] K. Albert, LC–NMR: Theory and Experiment, 1st ed., JohnWiley & Sons Ltd, Chichester, UK, 2002.

[7] W. Hiller, P. Sinha, M. Hehn, H. Pasch, Online LC-NMR – From an expensive toy to a powerful tool in polymer analysis, Prog. Polym. Sci. 39 (2014) 979–1016, https://doi.org/10.1016/j.progpolymsci.2013.10.001.

[8] M. Cudaj, G. Guthausen, T. Hofe, M. Wilhelm, Online coupling of size-exclusion chromatography and low-field $^{1}$H NMR spectroscopy, Macromol. Chem. Phys. 213 (2012) 1933–1943, https://doi.org/10.1002/macp.201200290.

[9] M. Matz, M. Pollard, M. Gaborieau, J. Tratz, C. Botha, M. Wilhelm, Enhancing sensitivity in the hyphenation of high-performance liquid chromatography to benchtop nuclear magnetic resonance spectroscopy at isocratic and onflow conditions, J. Phys. Chem. B 128 (2024) 9512–9524, https://doi.org/10.1021/acs.jpcb.4c03509.

[10] M. Gaborieau, M. Matz, J. Tratz, M. Pollard, M. Wilhelm, Online coupling of 80 MHz benchtop 2D-COSY NMR to HPLC, Macromol. Rapid. Commun. 46 (2025) 2500239, https://doi.org/10.1002/marc.202500239.

[11] T. Hofe, personal communication to M. Wilhelm, (21. July 2005).

[12] S.K. Küster, E. Danieli, B. Blümich, F. Casanova, High-resolution NMR spectroscopy under the fume hood, Phys. Chem. Chem. Phys. 13 (2011) 13172–13176, https://doi.org/10.1039/C1CP21180C.

[13] T. Castaing-Cordier, D. Bouillaud, J. Farjon, P. Giraudeau, Chapter four - recent advances in benchtop NMR spectroscopy and its applications, Annu. Rep. NMR Spectrosc 103 (2021) 191–258, https://doi.org/10.1016/bs.arnmr.2021.02.003.

[14] G. Zheng, W.S. Price, Solvent signal suppression in NMR, Prog. Nucl. Magn. Reson. Spectrosc. 56 (2010) 267–288, https://doi.org/10.1016/j.pnmrs.2010.01.001.

[15] B. Gouilleux, B. Charrier, S. Akoka, P. Giraudeau, Gradient-based solvent suppression methods on a benchtop spectrometer, Magn. Reson. Chem. 55 (2016) 91–98, https://doi.org/10.1002/mrc.4493.

[16] J. Pellizzari, R. Soong, K. Downey, R.G. Biswas, F.C. Kock, K. Steiner, B. Goerling, A. Haber, V. Decker, F. Busse, M. Simpson, A. Simpson, Slice through the water—Exploring the fundamental challenge of water suppression for Benchtop NMR systems, Magn. Reson. Chem. 62 (2024) 463–473, https://doi.org/10.1002/mrc.5431.

[17] J. Höpfner, B. Mayerhöfer, C. Botha, D. Bouillaud, J. Farjon, P. Giraudeau, M. Wilhelm, Solvent suppression techniques for coupling of size exclusion chromatography and $^{1}$H NMR using benchtop spectrometers at 43 and 62 MHz, J. Magn. Reson. 323 (2021) 106889, https://doi.org/10.1016/j.jmr.2020.106889.

[18] J.G. Proakis, D.G. Manolakis, The discrete fourier transform: its properties and applications, in: J.G. Proakis, D.G. Manolakis (Eds.), Digital Signal Processing, Pearson International, Essex, 2013, pp. 449–502.

[19] J. Schlagnitweit, S.W. Morgan, M. Nausner, N. Müller, H. Desvaux, Non-linear signal detection improvement by radiation damping in single-pulse NMR spectra, Chem. Phys. Chem. 13 (2012) 482–487, https://doi.org/10.1002/cphc.201100724.

[20] D.I. Hoult, Solvent peak saturation with single phase and quadrature fourier transformation, J. Magn. Reson. 21 (1976) 337–347, https://doi.org/10.1016/0022-2364(76)90081-0.

[21] J. Jesson, P. Meakin, G. Kneissel, Homonuclear decoupling and peak elimination in fourier transform nuclear magnetic resonance, J. Am. Chem. Soc. 95 (1973) 618–620, https://doi.org/10.1021/ja00783a068.

[22] P. Plateau, M. Gueron, Exchangeable Proton NMR without base-line distorsion, using new strong-pulse sequences, J. Am. Chem. Soc. 104 (1982) 7310–7311, https://doi.org/10.1021/ja00389a067.

[23] R.J. Ogg, R.B. Kingsley, J.S. Taylor, WET, a T1- and B1-insensitive water-suppression method for in vivo localized 1H NMR spectroscopy, J. Magn. Reson. Ser. B 104 (1994) 1–10, https://doi.org/10.1006/jmrb.1994.1048.

[24] M. Piotto, V. Saudek, V. Sklenár, Gradient-tailored excitation for single-quantum NMR spectroscopy of aqueous solutions, J. Biomol. NMR 2 (1992) 661–665, https://doi.org/10.1007/BF02192855.

[25] B. Gouilleux, J. Farjon, P. Giraudeau, Gradient-based pulse sequences for benchtop NMR spectroscopy, J. Magn. Reson. 319 (2020) 106810, https://doi.org/10.1016/j.jmr.2020.106810.

[26] T.E. Skinner, J. Pruski, P.-M.L. Robitaille, Solvent suppression using a rise-time-compensated high-pass filter, J. Magn. Res. 98 (1992) 604–607, https://doi.org/10.1016/0022-2364(92)90012-V.

[27] G. Zheng, A.M. Torres, W.S. Price, WaterControl: self-diffusion based solvent signal suppression enhanced by selective inversion, Magn. Reson. Chem. 55 (2017) 447–451, https://doi.org/10.1002/mrc.4420.

[28] P.C.M. van Zijl, C.T.W. Moonen, Complete water suppression for solutions of large molecules based on diffusional differences between Solute and Solvent (DRYCLEAN), J. Magn. Reson. 87 (1990) 18–25, https://doi.org/10.1016/0022-2364(90)90082-K.

[29] R. Mills, Self-diffusion in normal and heavy water in the range 1-45.deg, J. Phys. Chem. 77 (1973) 685–688, https://doi.org/10.1021/j100624a025.

[30] G. Fleischer, The chain length dependence of self-diffusion in melts of polyethylene and polystyrene, Colloid Polym. Sci. 265 (1987) 89–95, https://doi.org/10.1007/BF01412750.

[31] A.M. Asoltanei, E.T. Iacob-Tudose, M.S. Secula, I. Mamaliga, Mathematical models for estimating diffusion coefficients in concentrated polymer solutions from experimental data, Processes 12 (2024) 1266, https://doi.org/10.3390/pr12061266.

[32] S.H. Donaldson Jr., J.P. Jahnke, R.J. Messinger, Å. Östlund, D. Uhrig, J. N. Israelachvili, B.F. Chmelka, Correlated diffusivities, solubilities, and hydrophobic interactions in ternary polydimethylsiloxane–Water–Tetrahydrofuran mixtures, Macromolecules 49 (2016) 6910–6917, https://doi.org/10.1021/acs.macromol.6b01514.

[33] Z. Gong, J.D. Walls, Diffusion selective pulses, J. Phys. Chem. Lett. 11 (2020) 456–462, https://doi.org/10.1021/acs.jpclett.9b03222.

[34] J. Höpfner, K.-F. Ratzsch, C. Botha, M. Wilhelm, Medium resolution $^{1}$HNMR at 62 MHz as a new chemically sensitive online detector for size-exclusion chromatography (SEC–NMR), Macromol. Rapid. Commun. 39 (2018) 1700766, https://doi.org/10.1002/marc.201700766.

[35] S.L. Patt, B.D. Sykes, Water eliminated fourier transform NMR spectroscopy, J. Chem. Phys. 56 (1972) 3182–3184, https://doi.org/10.1063/1.1677669.

[36] C. Botha, J. Höpfner, B. Mayerhöfer, M. Wilhelm, On-line SEC-MR-NMR hyphenation: optimization of sensitivity and selectivity on a 62 MHz benchtop NMR spectrometer, Polym. Chem. 10 (2019) 2230–2246, https://doi.org/10.1039/C9PY00140A.

[37] M. Matz, Ph.D. thesis: entwicklung und optimierung von methoden zur sensitivitätssteigerung in der HPLC-benchtop NMR Kopplung, Karlsruher Institut für Technologie (KIT), Karlsruhe, Germany, 2024.

[38] E. Danieli, J. Perlo, B. Blümich, F. Casanova, Small magnets for portable NMR spectrometers, Angew. Chem. Int. Ed. 49 (2010) 4133–4135, https://doi.org/10.1002/anie.201000221.

[39] H. Mo, D. Raftery, Pre-SAT180, a simple and effective method for residual water suppression, J. Magn. Res. 190 (2008) 1–6, https://doi.org/10.1016/j.jmr.2007.09.016.

[40] S. Zhang, X. Yang, D.G. Gorenstein, Enhanced suppression of residual water in a "270" WET sequence, J. Magn. Res. 143 (2000) 382–386, https://doi.org/10.1006/jmre.1999.1987.

[41] G.H. Sørland, Pulsed field gradient—NMR sequences, in: G.H. Sørland (Ed.), Dynamic Pulsed-Field-Gradient NMR, Springer Berlin Heidelberg, Berlin, Heidelberg, 2014, pp. 1–35.

[42] C.B. Botha, Ph.D. thesis: method development of new chemically sensitive detectors for size exclusion chromatography, Karlsruher Institut für Technologie (KIT), Karlsruhe, Germany, 2021.

[43] J. Tratz, M. Gaborieau, M. Matz, M. Pollard, M. Wilhelm, Potential of benchtop NMR for the determination of polymer molar masses, molar mass distributions, and chemical composition profiles by means of diffusion-ordered spectroscopy, DOSY, macromol, Rapid Commun. (2024) e2400512, https://doi.org/10.1002/marc.202400512.

[44] T. Ye, C. Zheng, S. Zhang, G.A. Gowda, O. Vitek, D. Raftery, Add to subtract": a simple method to remove complex background signals from the 1H nuclear magnetic resonance spectra of mixtures, Anal. Chem. 84 (2012) 994–1002, https://doi.org/10.1021/ac202548n.

[45] C.K. Georgantopoulos, M.K. Esfahani, C. Botha, M.A. Pollard, I.F.C. Naue, A. Causa, R. Kádár, M. Wilhelm, Modeling the spatial characteristics of extrusion flow instabilities for styrene-butadiene rubbers: investigating the influence of molecular weight distribution, molecular architecture, and temperature, Phys. Fluids 33 (2021) 093108, https://doi.org/10.1063/5.0061334.

[46] W. Hiller, M. Hehn, T. Hofe, K. Oleschko, Online size exclusion chromatography−NMR for the determination of molar mass distributions of copolymers, Anal. Chem. 82 (2010) 8244–8250, https://doi.org/10.1021/ac1013095.

[47] P. Giraudeau, V. Silvestre, S. Akoka, Optimizing water suppression for quantitative NMR-based metabolomics: a tutorial review, Metabolomics 11 (2015), https://doi.org/10.1007/s11306-015-0794-7.

[48] S.H. Smallcombe, S.L. Patt, P.A. Keifer, WET solvent suppression and its applications to LC NMR and high-resolution NMR spectroscopy, J. Magn. Reson. Ser. A 117 (1995) 295–303, https://doi.org/10.1006/jmra.1995.0759.